Global Journal of Science Frontier Research
Physics and Space Science
Volume 13 Issue 6 Version 1.0 Year 2013
Type : Double Blind Peer Reviewed International Research Journal
Publisher: Global Journals Inc. (USA)
Online ISSN: 2249-4626 & Print ISSN: 0975-5896

Natural Convection of Heat Transfer in a Vertical Conical Annular Porous Medium

By Dr. D. Prabhakar & Dr. G. Prabhakararao
Fire Institution, India

Abstract - In this chapter, we study the natural convection heat transfer in a saturated porous medium confined in a vertical annular porous medium. In this study Finite Element Method (FEM) has been used to solve governing partial differential equations. Results are presented interms of average Nusselt number ($\bar{N}u$), streamlines and Isothermal lines for various values of Rayleigh number (Ra), Cone angle (C_A) and Radius ratio (R_r).

Keywords : *porous medium, pressure, Rayleigh number, boundary-layer, flux.*

GJSFR-A Classification : *FOR Code: 091505*

Strictly as per the compliance and regulations of :

© 2013. Dr. D. Prabhakar & Dr. G. Prabhakararao. This is a research/review paper, distributed under the terms of the Creative Commons Attribution-Noncommercial 3.0 Unported License http://creativecommons.org/licenses/by-nc/3.0/), permitting all non commercial use, distribution, and reproduction in any medium, provided the original work is properly cited.

Natural Convection of Heat Transfer in a Vertical Conical Annular Porous Medium

Dr. D. Prabhakar[α] & Dr. G. Prabhakararao[σ]

Abstract - In this chapter, we study the natural convection heat transfer in a saturated porous medium confined in a vertical annular porous medium. In this study Finite Element Method (FEM) has been used to solve governing partial differential equations. Results are presented interms of average Nusselt number ($\bar{N}u$), streamlines and Isothermal lines for various values of Rayleigh number (Ra), Cone angle (C_A) and Radius ratio (R_r).

Keywords : porous medium, pressure, Rayleigh number, boundary-layer, flux.

I. Introduction

Natural convection heat transfer in a saturated porous medium has a number of important and geophysical applications, such as nuclear reactor cooling system and underground energy transport. The problems of free convection about a vertical impermeable flat plate are studied by cheng and Minkowycz [1], Cheng [2], Na and Pop [3] Gorla and Zinalabedini [4]. The vertical cylinder cases are investigated by Minkowycz and Cheng [5], Kumari etal [6], Markin [7] and Basson et.al [8] Cheng et al. [9] use the local non-similarity method to analyze the natural convection of Darcial fluid about a cone.

The effect of surface mass flux on a vertical flat plate [10] the similarity solution is possible only when the variations of the wall temperature and the transpiration rate are proportional to power-law of x measured from the leading edge.

From practical point of view, however, the uniform mass flux may be easily realized. The effect of uniform surface mass flux on a vertical flat plate with uniform wall temperature is investigated by Merkin [11] and Minkowycz and Cheng [12]. Yücel [13], and Hwang and Chen [14] numerically study the vertical cylinder case.

Khan and Zebib [15] studied the double – diffusive instability of the double boundary – layer structure that forms near a vertical wall immersed in temperature and concentration stratified porous medium. Raptis et al. [16] constructed similarity solutions of boundary - layer near a vertical surface wall in porous medium with constant temperature and concentration. Bejan and Khair [17] used Darcy's law to study the vertical natural convective flows driven by temperature and concentration gradients. Lal and Kulacki [18] studied the natural convection boundary layer flow along a vertical surface with constant heat and mass flux including the effect of wall injection. Nakayama and Hossain [19], and Singh and Queeny [20] applied the integral method to obtain the heat and mass transfer by free convection from a vertical surface with constant wall temperature and concentration. Yih [21] studied the heat and mass transfer characteristics in natural convection flow over a truncated cone subjected to variable wall temperature and concentration or variable heat and mass flux embedded in porous medium.

Comprehensive review on this phenomenon has been recently reported by Trevisan and Bejan [22] for various geometries. Bejan and khair [23] investigated the vertical natural convection boundary – layer flow in a saturated porous medium due to the combined heat and mass transfer. Jang and Chang [24] studied the buoyancy – induced inclined boundary - layer in porous medium resulting from combined heat and mass buoyancy effects.

Heat and mass transfer about vertical cylinder in saturated porous media is analyzed by Yücel [25] [26]. Nakayama and Hossain [27], and Singh and Queeny [28] used an integral method to solve the problem of Bejan and khair [23]. Lai et al [29] investigated the coupled heat and mass transfer by natural convection from horizontal line sources in saturated porous media. Nakayama and Ashizawa [32] performed a boundary layer analysis of combined heat and mass transfer by natural convection from a concentrated source in a saturated porous medium.

In this chapter, we study the natural convection heat transfer in a saturated porous medium confined in a vertical annular porous medium. In this study Finite Element Method (FEM) has been used to solve governing partial differential equations. Results are presented interms of average Nusselt number ($\bar{N}u$), streamlines and Isothermal lines for various values of Rayleigh number (Ra), Cone angle (C_A) and Radius ratio (R_r).

II. Mathematical Formulation

A vertical annular cone of inner radius ri and outer radius r_0 as depicted by schematic diagram as shown in figure (A) is considered to investigate the heat transfer behavior. The co-ordinate system is chosen

Author α : Department of Fire Office, Yemmiganuru, Kurnool-District-Andhra Pradesh-India. E-mail : dprabhakar1234@gmail.com
Author σ : Lecturer in Mathematics SVGM Government Degree College, Kalyandurg, Anantapur-Dist, Andhra Pradesh-India.
E-mail : nari.prabhu@gmail.com

© 2013 Global Journals Inc. (US)

such that the r-axis points towards the width and z-axis towards the height of the cone respectively. Because of the annular nature, two important parameters emerge which are Cone angle (C_A) and Radius ratio (R_r) of the annulus. They are defined as

$$C_A = \frac{H_t}{r_0 - r_i}, \quad R_r = \frac{r_0 - r_i}{r_i}$$

where H_t is the height of the cone.

The inner surface of the cone is maintained at isothermal temperature T_h and outer surface is at ambient temperature T_∞. It may be noted that, due to axisymmetry, only a section on the annulus is sufficient for analysis purpose.

Following assumptions are made:

- The flow inside the porous medium obeys Darcy law and there is no phase change of fluid.
- Porous medium is saturated with fluid.
- The fluid and medium are in local thermal equilibrium in the domain.
- The porous medium is isotropic and homogeneous.
- Fluid properties are constant except the variation of density.

With the above assumptions, the governing equations are given by continuity equation:

$$\frac{\partial(ru)}{\partial r} + \frac{\partial(rw)}{\partial z} = 0 \qquad (1.2.1)$$

The velocity in r and z directions can be described by Darcy law as
Velocity in horizontal direction

$$u = \frac{-K}{\mu}\frac{\partial p}{\partial r} \qquad (1.2.2)$$

velocity in vertical direction

$$w = \frac{-K}{\mu}\left(\frac{\partial p}{\partial z} + \rho g\right) \qquad (1.2.3)$$

the permeability K of porous medium can be expressed as Bejan (33)

$$K = \frac{D_p^2 \phi^3}{180(1-\phi)^2} \qquad (1.2.4)$$

The variation of density with respect to temperature can be described by Boussinesq approximation as

$$\rho = \rho_\infty [\, 1 - \beta_T (T - T_\infty) \qquad (1.2.5)$$

Momentum Equation:

$$\frac{\partial w}{\partial r} - \frac{\partial u}{\partial z} = \frac{gK\beta}{\nu}\frac{\partial T}{\partial r} \qquad (1.2.6)$$

Energy equation:

$$u\frac{\partial T}{\partial r} + w\frac{\partial T}{\partial z} = \alpha\left(\frac{1}{r}\frac{\partial}{\partial r}\left(r\frac{\partial T}{\partial r}\right) + \frac{\partial^2 T}{\partial z^2}\right) \qquad (1.2.7)$$

The continuity equation (1.2.1) can be satisfied by introducing the stream function ψ as

$$u = -\frac{1}{r}\frac{\partial \psi}{\partial z} \qquad (1.2.8)$$

$$w = \frac{1}{r}\frac{\partial \psi}{\partial r} \qquad (1.2.9)$$

The corresponding dimensional boundary conditions are

$$\text{at} \quad r = r_i\,, \quad T = T_w\,, \quad \psi = 0 \qquad (1.2.10a)$$

$$\text{at} \quad r = r_0\,, \quad T = T_\infty\,, \quad \psi = 0 \qquad (1.2.10b)$$

(except at z = 0)

The new parameters arising due to cylindrical co-ordinates system are
Non-dimensional Radius

$$\bar{r} = \frac{r}{L} \qquad (1.2.11a)$$

Non-dimensional Height

$$\bar{z} = \frac{z}{L} \qquad (1.2.11b)$$

Non-dimensional stream function

$$\bar{\psi} = \frac{\psi}{\alpha L} \qquad (1.2.11c)$$

Non-dimensional Temperature

$$\bar{T} = \frac{(T - T_\infty)}{(T_w - T_\infty)} \qquad (1.2.11d)$$

Rayleigh number

$$Ra = \frac{g\beta_T \Delta T K L}{\nu\alpha} \qquad (1.2.11e)$$

The non-dimensional equations for the heat transfer in vertical cone are

Momentum equation:

$$\frac{\partial^2 \bar{\psi}}{\partial \bar{z}^2} + \bar{r}\left(\frac{1}{\bar{r}}\frac{\partial \bar{\psi}}{\partial \bar{r}}\right) = \bar{r} Ra \frac{\partial \bar{T}}{\partial \bar{r}}$$

© 2013 Global Journals Inc. (US)

Energy equation:

$$\frac{1}{\bar{r}}\left[\frac{\partial\bar{\psi}}{\partial\bar{r}}\frac{\partial\bar{T}}{\partial\bar{z}}-\frac{\partial\bar{\psi}}{\partial\bar{z}}\frac{\partial\bar{T}}{\partial\bar{r}}\right]=\left(\frac{1}{\bar{r}}\frac{\partial}{\partial\bar{r}}\left(\bar{r}\frac{\partial\bar{T}}{\partial\bar{r}}\right)+\frac{\partial^2\bar{T}}{\partial\bar{z}^2}\right) \quad (1.2.13)$$

The corresponding non-dimensional boundary conditions are

$$\text{at} \quad \bar{r}=\bar{r}_i, \qquad \bar{T}=1, \quad \bar{\psi}=0 \quad (1.2.14)$$

$$\text{at} \quad \bar{r}=\bar{r}_0, \qquad \bar{T}=0, \quad \bar{\psi}=0 \quad (1.2.15)$$

III. Solution of Governing Equations

The partial differential equations, which describe the heat and fluid flow behavior in the vicinity of porous medium are given earlier. There are various numerical methods available to achieve the solution of these equations, but the most popular numerical methods are Finite difference method, Finite volume method and the Finite element method. The selection of these numerical methods is an important decision, which is influenced by variety of factors amongst which the geometry of domain plays a vital role. Other factors include the ease with which these partial differential equations can be transformed into simple forms, the computational time required and the flexibility in development of computer code to solve these equations.

In the present study, we have used Finite Element Method (FEM). The following sections briefly described the Finite Element Method and present its application to solve the above mentioned equations.

The Finite Element Method is a popular method amongst scientific community. This method was originally developed to study the mechanical stresses in a complex air frame structure Clough (36) and popularized by Zienkiewicz and Cheung (37) by applying it to continuum mechanics. Since then the application of finite element method has been exploited to solve the numerous problems in various engineering disciplines.

The great thing about finite element method is its ease with which it can be generalized to engineering problems comprised of different materials. Another admirable feature of the Finite Element Method (FEM) is that it can be applied to wide range of geometries having irregular boundaries, which is highly difficult to achieve with other contemporary methods. FEM can be said to have comprised of roughly 5 steps to solve any particular problem. The steps can be summarized as :

- Descritizing the domain: This step involves the division of whole physical domain into smaller segments known as elements, and then identifying the nodes, coordinates of each node and ensuring proper connectivity between the nodes.
- Obtaining the characteristics of the element which is written in terms of nodal values
- Development of Global matrix: The equations are arranged in a global matrix which takes into account the whole domain
- Solution: The equations are solved to get the desired variable at each node in the domain
- Evaluate the quantities of interest: After solving the equations a set of values are obtained for each node, which can be further processed to get the quantities of interest.

There are varieties of elements available in FEM, which are distinguished by the presence of number of nodes. The present study is carried out by using a simple 3- noded triangular element as shown in figure (1).

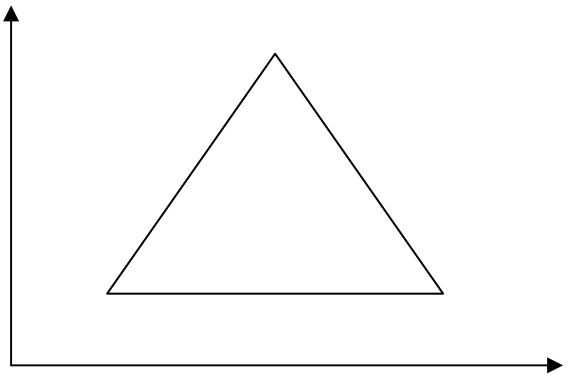

Figure 1 : Typical triangular element

Let us consider that the variable to be determined in the triangular area as "T".
The polynomial function for "T" can be expressed as:

$$T = \alpha_1 + \alpha_2 r + \alpha_3 z \quad (1.2.15)$$

The variable T has the value T_i, T_j & T_k at the nodal position i, j & k of the element. The r and z co-ordinates at these points are r_i, r_j, r_k and z_i, z_j, z_k respectively. Substitution of these nodal values in the equation (1.2.15) helps in determining the constants a_1, a_2 , a_3 which are:

$$\alpha_i = {}^1/_{2A}\left[(r_j z_k - r_k z_j) T_i + (r_k z_i - r_i z_k) T_j + (r_i z_j - r_j z_i) T_k\right] \quad (1.2.16)$$

$$\alpha_2 = {}^1/_{2A}\left[(z_j - z_k) T_i + (z_k - z_i) T_j + (z_i - z_j) T_k\right] \quad (1.2.17)$$

$$\alpha_3 = {}^1/_{2A}\left[(r_k - r_j) T_i + (r_i - r_k) T_j + (r_j - r_i) T_k\right] \quad (1.2.18)$$

© 2013 Global Journals Inc. (US)

where A is area of the triangle given as

$$2A = \det\begin{vmatrix} 1 & r_i & z_i \\ 1 & r_j & z_j \\ 1 & r_k & z_k \end{vmatrix} \quad (1.2.19)$$

Substitution of a_1, a_2, a_3 in the equation (1.2.15) and mathematical arrangement of the terms results into

The constants can be expressed in terms of coordinates as

$$\left.\begin{array}{ll} a_i = r_j z_k - r_k z_j & b_i = z_j - z_k \\ a_j = r_k z_i - r_i z_k & b_j = z_k - z_i \\ a_k = r_i z_j - r_j z_i & b_k = z_i - z_j \end{array} \quad \begin{array}{ll} c_i = r_k - r_j \\ c_j = r_i - r_k \\ c_k = r_j - r_i \end{array}\right\} \quad (1.2.22)$$

Good insight into the FEM is given in Segerland (35); Elshayed and Beng (33) Lewis et al. (34). Galerkin method is employed to convert the partial differential equations into matrix form of equation for an element. The steps involved are as given below.

Please note that the nodal terms *i, j & k* are replaced by 1,2 & 3 respectively in subsequent discussions for simplicity.

Applying of Galerkin method to momentum equation (1.2.12) yields

$$\{R^e\} = -\int_A N^T \left(\frac{\partial^2 \bar{\psi}}{\partial \bar{z}^2} + \bar{r} \frac{\partial}{\partial \bar{r}} \left(\frac{1}{\bar{r}} \frac{\partial \bar{\psi}}{\partial \bar{r}} \right) + \bar{r} Ra \frac{\partial \bar{T}}{\partial \bar{r}} \right) d\nu \quad (1.2.23)$$

$$T = N_i T_i + N_j T_j + N_k T_k \quad (1.2.20)$$

In equation (1.2.20) N_i, N_j, N_k are the shape functions give by

$$N_m = \frac{a_m + b_m r + c_m z}{2A}, \text{m} = \text{i, j \& k} \quad (1.2.21)$$

$$\{R^e\} = -\int_A N^T \left(\frac{\partial^2 \bar{\psi}}{\partial \bar{z}^2} + \bar{r} \frac{\partial}{\partial \bar{r}} \left(\frac{1}{\bar{r}} \frac{\partial \bar{\psi}}{\partial \bar{r}} \right) + \bar{r} Ra \frac{\partial \bar{T}}{\partial \bar{r}} \right) 2\Pi \bar{r} dA \quad (1.2.24)$$

where R^e is the residue. Considering individual terms of equation (1.2.24)

The differentiation of following term results into

$$\frac{\partial}{\partial \bar{r}} \left([N^T] \frac{\partial \bar{\psi}}{\partial \bar{r}} \right) = [N^T] \frac{\partial^2 \bar{\psi}}{\partial \bar{r}^2} + \frac{\partial [N^T]}{\partial \bar{r}} \frac{\partial \bar{\psi}}{\partial \bar{r}} \quad (1.2.25)$$

Thus

$$\int_A N^T \frac{\partial^2 \bar{\psi}}{\partial \bar{r}^2} dA = \int_A \frac{\partial}{\partial \bar{r}} \left([N^T] \frac{\partial^2 \bar{\psi}}{\partial \bar{r}^2} \right) 2\Pi \bar{r} dA - \int_A \frac{\partial [N^T]}{\partial \bar{r}} \frac{\partial \bar{\psi}}{\partial \bar{r}} \quad (1.2.26)$$

The first term on right hand side of equation (1.2.26) can be transformed into surface integral by the application of Greens theorem and leads to inter-element requirement at boundaries of an element. The boundary conditions are incorporated in the force vector.

Making use of (1.2.20) produces

$$\int_A N^T \frac{\partial^2 \bar{T}}{\partial \bar{r}^2} 2\Pi \bar{r} dA = -\int_A \frac{\partial N^T}{\partial \bar{r}} \frac{\partial N}{\partial \bar{r}} \begin{Bmatrix} \bar{\psi}_1 \\ \bar{\psi}_2 \\ \bar{\psi}_3 \end{Bmatrix} dA \quad (1.2.27)$$

Substitution of (1.2.21) into (1.2.27) gives

$$= \frac{-1}{(2A)^2} \int_A \begin{bmatrix} b_1 \\ b_2 \\ b_3 \end{bmatrix} [b_1 b_2 b_3] \begin{Bmatrix} \bar{\psi}_1 \\ \bar{\psi}_2 \\ \bar{\psi}_3 \end{Bmatrix} 2\Pi \bar{r} dA$$

$$= -\frac{2\Pi \bar{R}}{4A} \begin{bmatrix} b_1^2 & b_1 b_2 & b_1 b_3 \\ b_1 b_2 & b_2^2 & b_2 b_3 \\ b_1 b_3 & b_2 b_3 & b_3^2 \end{bmatrix} \begin{Bmatrix} \bar{\psi}_1 \\ \bar{\psi}_2 \\ \bar{\psi}_3 \end{Bmatrix} \quad (1.2.28)$$

Similarly

$$\int_A N^T \frac{\partial^2 \bar{\psi}}{\partial \bar{z}^2} 2\Pi \bar{r} \, dA = -\frac{2\Pi \bar{R}}{4A} \begin{bmatrix} c_1^2 & c_1 c_2 & c_1 c_3 \\ c_1 c_2 & c_2^2 & c_2 c_3 \\ c_1 c_2 & c_2 c_3 & c_3^2 \end{bmatrix} \begin{Bmatrix} \bar{\psi}_1 \\ \bar{\psi}_2 \\ \bar{\psi}_3 \end{Bmatrix} \quad (1.2.29)$$

© 2013 Global Journals Inc. (US)

The third term of equation (1.2.24) is

$$\int_A N^T \bar{r} Ra \frac{\partial \bar{T}}{\partial \bar{r}} \; \bar{\Pi} \bar{r} dA = Ra \int_A N^T \bar{r} \frac{\partial \bar{T}}{\partial \bar{r}} 2\bar{\Pi} \bar{r} dA \tag{1.2.30}$$

In order to get the matrix equation of (1.2.30), the following method can be applied. The triangular element can be subdivided into three triangles with a point in the center of original triangle as shown in figure (2).

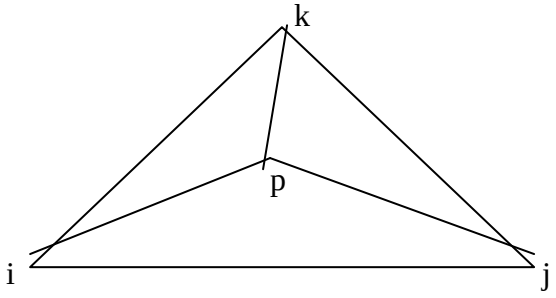

Figure 2 : Showing the sub triangular areas

Defining the new area ratios as

$$M_k = \frac{area \;\; pij}{area \;\; ijk} \qquad M_i = \frac{area \;\; pjk}{area \;\; ijk} \qquad M_j = \frac{area \;\; pki}{area \;\; ijk}$$

It can be shown Elshyab and Beng (33) that

$$M_i = N_1 \qquad M_j = N_2 \qquad M_k = N_3 \tag{1.2.31}$$

Replacing shape functions in equation (1.2.30) by (1.1.31) yields

$$\int_A N^T \bar{r} Ra \frac{\partial \bar{T}}{\partial \bar{r}} 2\bar{\Pi} \bar{r} dA = \bar{r} Ra \int_A \begin{bmatrix} M_1 \\ M_2 \\ M_3 \end{bmatrix} \frac{\partial (N)}{\partial \bar{r}} \begin{bmatrix} \bar{T}_1 \\ \bar{T}_2 \\ \bar{T}_3 \end{bmatrix} 2\bar{\Pi} \bar{r} dA \tag{1.2.32}$$

The area integration can be evaluated by a simple relation Segerland (35).

$$\int_A M_1^d M_2^e M_3^f = \frac{d!e!f!}{(d+e+f+2)!} 2A \tag{1.2.33}$$

Application of equation (1.2.33) into (1.2.32) gives rise to:

$$= Ra \frac{A}{3} \begin{bmatrix} 1 \\ 1 \\ 1 \end{bmatrix} \frac{2\bar{\Pi} \bar{R}^2}{2A} \left[b_1 + b_2 + b_3 \right] \begin{bmatrix} \bar{T}_1 \\ \bar{T}_2 \\ \bar{T}_3 \end{bmatrix} \tag{1.2.34}$$

$$= \frac{2\bar{\Pi} \bar{R}^2 Ra}{6} \begin{Bmatrix} b_1 \bar{T}_1 + b_2 \bar{T}_2 + b_3 \bar{T}_3 \\ b_1 \bar{T}_1 + b_2 \bar{T}_2 + b_3 \bar{T}_3 \\ b_1 \bar{T}_1 + b_2 \bar{T}_2 + b_3 \bar{T}_3 \end{Bmatrix} \tag{1.2.35}$$

Now the momentum equation (1.2.12) can be written in the matrix form as

$$\frac{2\bar{\Pi} \bar{R}}{4A} \left\{ \begin{bmatrix} b^2 & b_1 b_2 & b_1 b_3 \\ b_1 b_2 & b_2^2 & b_2 b_3 \\ b_1 b_3 & b_2 b_3 & b_3^2 \end{bmatrix} + \begin{bmatrix} c_1^2 & c_1 c_2 & c_1 c_3 \\ c_1 c_2 & c_2^2 & c_2 c_3 \\ c_1 c_2 & c_2 c_3 & c_3^2 \end{bmatrix} \right\} \begin{Bmatrix} \bar{\psi}_1 \\ \bar{\psi}_2 \\ \bar{\psi}_3 \end{Bmatrix} + \frac{2\bar{\Pi} \bar{R}^2 Ra}{6} \begin{Bmatrix} b_1 \bar{T}_1 + b_2 \bar{T}_2 + b_3 \bar{T}_3 \\ b_1 \bar{T}_1 + b_2 \bar{T}_2 + b_3 \bar{T}_3 \\ b_1 \bar{T}_1 + b_2 \bar{T}_2 + b_3 \bar{T}_3 \end{Bmatrix} = 0 \tag{1.2.36}$$

In simple form the above equation can be represented as:

$$[K_s] \{ \bar{\psi} \} = \{ f \} \tag{1.2.37}$$

where K_S is stiffness matrix and f is the force vector. For equation (1.2.12) they are:

$$[K_s] = \frac{2\bar{\Pi} \bar{R}}{4A} \left\{ \begin{bmatrix} b_1^2 & b_1 b_2 & b_1 b_3 \\ b_1 b_2 & b_2^2 & b_2 b_3 \\ b_1 b_3 & b_2 b_3 & b_3^2 \end{bmatrix} + \begin{bmatrix} c_1^2 & c_1 c_2 & c_1 c_3 \\ c_1 c_3 & c_2 c_3 & c_3^2 \end{bmatrix} \right\} \tag{1.2.38a}$$

© 2013 Global Journals Inc. (US)

$$\{\bar{\psi}\} = \begin{Bmatrix} \bar{\psi}_1 \\ \bar{\psi}_2 \\ \bar{\psi}_3 \end{Bmatrix} \tag{1.2.38b}$$

$$\{f\} = \frac{2\Pi \bar{R}^2 Ra}{6} \begin{Bmatrix} b_1\bar{T}_1 + b_2\bar{T}_2 + b_3\bar{T}_3 \\ b_1\bar{T}_1 + b_2\bar{T}_2 + b_3\bar{T}_3 \\ b_1\bar{T}_1 + b_2\bar{T}_2 + b_3\bar{T}_3 \end{Bmatrix} \tag{1.2.38c}$$

The radial distance $\bar{R}$ to the centroid of an element is given by relation

$$\bar{R} = \frac{\bar{r}_1 + \bar{r}_2 + \bar{r}_3}{3}$$

Similarly application of Galerkin method to Energy equation (1.2.13) gives

$$\{R^e\} = -\int_A [N]^T \left[\frac{1}{\bar{r}} \left(\frac{\partial \bar{\psi}}{\partial \bar{r}} \frac{\partial \bar{T}}{\partial \bar{z}} - \frac{\partial \bar{\psi}}{\partial \bar{z}} \frac{\partial \bar{T}}{\partial \bar{r}} \right) - \left(\frac{1}{\bar{r}} \frac{\partial}{\partial \bar{r}} \left\{ \bar{r} \frac{\partial \bar{T}}{\partial \bar{r}} \right\} + \frac{\partial^2 \bar{T}}{\partial \bar{z}^2} \right) \right] 2\Pi \bar{r} dA \tag{1.2.39}$$

Considering the terms individually of the above equation

$$\int_A [N]^T \frac{\partial \bar{\psi}}{\partial \bar{z}} \frac{\partial \bar{T}}{\partial \bar{r}} 2\Pi dA = \int_A \begin{bmatrix} M_1 \\ M_2 \\ M_3 \end{bmatrix} \frac{\partial [N]}{\partial \bar{z}} \{\bar{\psi}\} \frac{\partial [N]}{\partial \bar{r}} \{\bar{T}\} 2\Pi \bar{r} dA \tag{1.2.40}$$

$$= \frac{2\Pi A}{3} \mathrm{X} \frac{1}{4A^2} \left[c_1\bar{\psi}_1 + c_2\bar{\psi}_2 + c_3\bar{\psi}_3 \right] \left[b_1, b_2, b_3 \right] \begin{bmatrix} \bar{T}_1 \\ \bar{T}_2 \\ \bar{T}_3 \end{bmatrix} \tag{1.2.41}$$

$$= \frac{2\Pi}{12A} \begin{Bmatrix} c_1\bar{\psi}_1 + c_2\bar{\psi}_2 + c_3\bar{\psi}_3 \\ c_1\bar{\psi}_1 + c_2\bar{\psi}_2 + c_3\bar{\psi}_3 \\ c_1\bar{\psi}_1 + c_2\bar{\psi}_2 + c_3\bar{\psi}_3 \end{Bmatrix} \left[b_1, b_2, b_3 \right] \begin{bmatrix} \bar{T}_1 \\ \bar{T}_2 \\ \bar{T}_3 \end{bmatrix} \tag{1.2.42}$$

Following the same above steps

$$\int_A [N]^T \frac{\partial \bar{\psi}}{\partial \bar{r}} \frac{\partial \bar{T}}{\partial \bar{z}} 2\Pi dA = \int_A \begin{bmatrix} M_1 \\ M_2 \\ M_3 \end{bmatrix} \frac{\partial [N]}{\partial \bar{r}} \{\bar{\psi}\} \frac{\partial [N]}{\partial \bar{z}} \{\bar{T}\} 2\Pi dA$$

$$\int_A N^T \frac{\partial \bar{\psi}}{\partial \bar{r}} \frac{\partial \bar{T}}{\partial \bar{z}} 2\Pi dA = \frac{2\Pi}{12A} \begin{Bmatrix} b_1\bar{\psi}_1 + b_2\bar{\psi}_2 + b_3\bar{\psi}_3 \\ b_1\bar{\psi}_1 + b_2\bar{\psi}_2 + b_3\bar{\psi}_3 \\ b_1\bar{\psi}_1 + b_2\bar{\psi}_2 + b_3\bar{\psi}_3 \end{Bmatrix} \left[c_1, c_2, c_3 \right] \begin{bmatrix} \bar{T}_1 \\ \bar{T}_2 \\ \bar{T}_3 \end{bmatrix}$$

The remaining two terms of Energy equation can be evaluated in similar fashion of equation (1.2.24)

$$\int_A N^T \frac{1}{\bar{r}} \frac{\partial}{\partial \bar{r}} \left(\bar{r} \frac{\partial \bar{T}}{\partial \bar{r}} \right) 2\Pi \bar{r} dA = -\frac{2\Pi \bar{R}}{4A} \begin{bmatrix} b_1^2 & b_1b_2 & b_1b_3 \\ b_1b_2 & b_2^2 & b_2b_3 \\ b_1b_3 & b_2b_3 & b_3^3 \end{bmatrix} \begin{bmatrix} \bar{T}_1 \\ \bar{T}_2 \\ \bar{T}_3 \end{bmatrix}$$

© 2013 Global Journals Inc. (US)

$$\int_A N^T \frac{\partial^2 \bar{T}}{\partial \bar{z}^2} 2\Pi \bar{r} dA = -\frac{2\Pi \bar{R}}{4A} \begin{bmatrix} c_1^2 & c_1c_2 & c_1c_3 \\ c_1c_2 & c_2^2 & c_2c_3 \\ c_1c_3 & c_2c_3 & c_3^2 \end{bmatrix} \begin{bmatrix} \bar{T}_1 \\ \bar{T}_2 \\ \bar{T}_3 \end{bmatrix}$$

Thus the stiffness matrix of Energy equation is given by

$$\left[\frac{2\Pi}{12A} \begin{Bmatrix} c_1\bar{\psi}_1 + c_2\bar{\psi}_2 + c_3\bar{\psi}_3 \\ c_1\bar{\psi}_1 + c_2\bar{\psi}_2 + c_3\bar{\psi}_3 \\ c_1\bar{\psi}_1 + c_2\bar{\psi}_2 + c_3\bar{\psi}_3 \end{Bmatrix} [b_1, b_2, b_3] - \frac{2\Pi}{12A} \begin{Bmatrix} b_1\bar{\psi}_1 + b_2\bar{\psi}_2 + b_3\bar{\psi}_3 \\ b_1\bar{\psi}_1 + b_2\bar{\psi}_2 + b_3\bar{\psi}_3 \\ b_1\bar{\psi}_1 + b_2\bar{\psi}_2 + b_3\bar{\psi}_3 \end{Bmatrix} [c_1, c_2, c_3] \right] \begin{bmatrix} \bar{T}_1 \\ \bar{T}_2 \\ \bar{T}_3 \end{bmatrix}$$

$$+ \frac{2\Pi \bar{R}}{4A} \left\{ \begin{bmatrix} b_1^2 & b_1b_2 & b_1b_2 \\ b_1b_2 & b_2^2 & b_2b_3 \\ b_1b_3 & b_2b_3 & b_3^3 \end{bmatrix} \begin{bmatrix} \bar{T}_1 \\ \bar{T}_2 \\ \bar{T}_3 \end{bmatrix} + \begin{bmatrix} c_1^2 & c_1c_2 & c_1c_3 \\ c_1c_2 & c_2^2 & c_2c_3 \\ c_1c_3 & c_2c_3 & c_3^2 \end{bmatrix} \begin{bmatrix} \bar{T}_1 \\ \bar{T}_2 \\ \bar{T}_3 \end{bmatrix} \right\} = 0 \qquad (1.2.43)$$

IV. Results and Discussion

Results are obtained in terms of Nusselt number (Nu) at hot wall for various parameters such as Cone angle (C_A), Radius ratio (R_r) and Rayleigh number (Ra), when heat is supplied to vertical conical annular.

The average Nusselt number ($\bar{N}u$) is given by

$$\bar{N}u = \int_0^{\bar{z}} \left(\frac{\partial \bar{T}}{\partial \bar{r}} \right)$$

a)

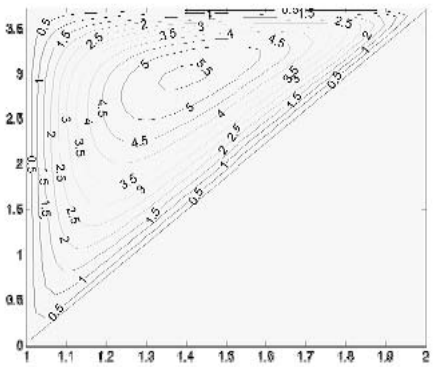

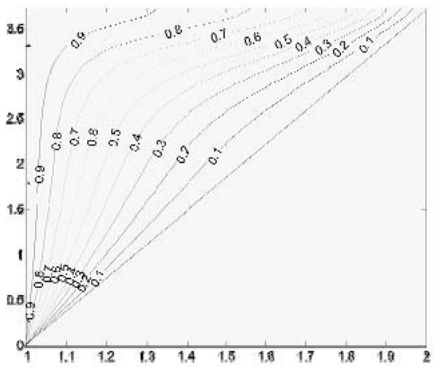

b)

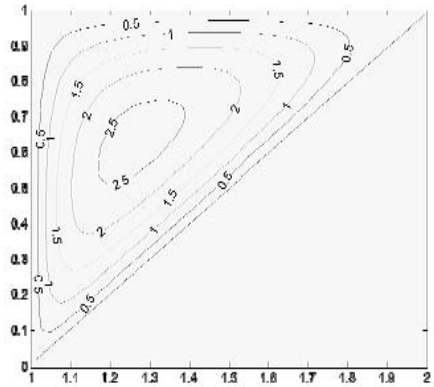

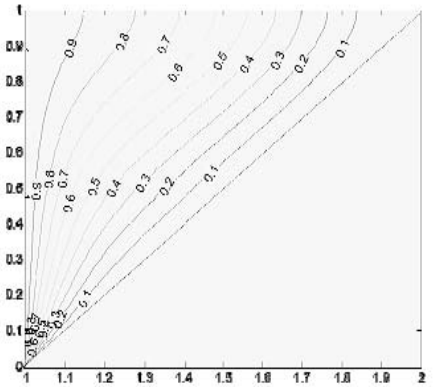

© 2013 Global Journals Inc. (US)

c)

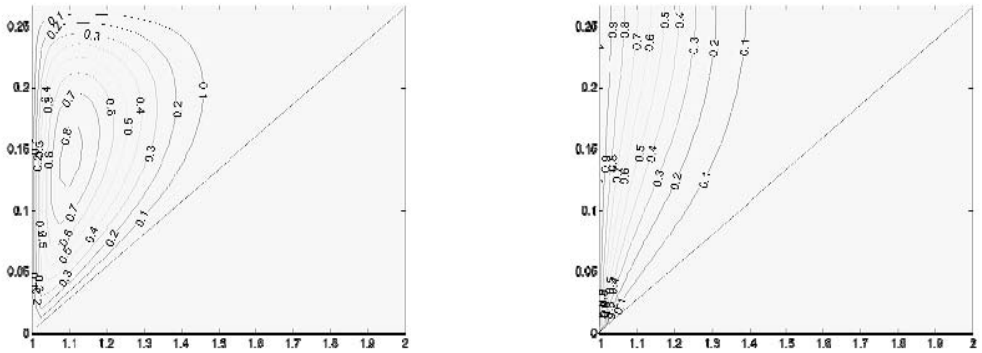

Figure 1.4.1 : Streamlines(left) and Isotherms(Right) for Ra=50, R_r=1
a) C_A =15 b) C_A =45 c) C_A =75

Figure (1.4.1) shows the evaluation of streamlines and isothermal lines inside the porous medium for various values of Cone angle (C_A) at Ra = 50, R_r = 1. The magnitude of the streamlines decreases with the increase in Cone angles (C_A). The thermal bounded layer thickness decreases with the increase of Cone angles (C_A). It can be seen from streamlines and isothermal lines that the fluid movements shifts from lower portion of the hot wall to upper portion of the cold wall of the vertical annual cone with the increase of Cone angles (C_A). The circulation of the fluid covers almost whole domain at both lower and higher values of Cone angles (C_A) at 15°. Where the relation inversely proportion exists between streamlines and Cone angles (C_A). This trend is also observed with isothermal lines.

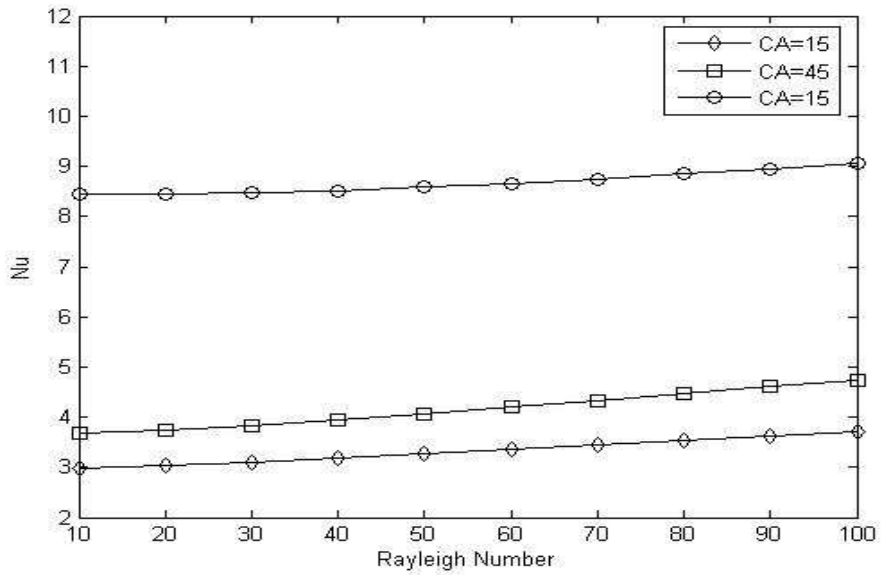

Figure 1.4.2 : $\bar{N}u$ variation with Ra at hot surface for different values of C_A at R_r=1

Figure (1.4.2) illustrates the effect of Rayleigh number (Ra) on the average Nusselt number ($\bar{N}u$). This Figure is obtained for value of R_r = 1. When cone angle is increased from 15 to 75, at the hot wall of the vertical annular cone, it is found that the average Nusselt number ($\bar{N}u$) at Ra = 10 is increased by 23.3%. The corresponding increase in average Nusselt number ($\bar{N}u$) at Ra = 100 is found to be 26.3%. The difference between the average Nusselt number ($\bar{N}u$) at two different values of Cone angle (C_A) increases with increase in Cone angle (C_A). This is due to the reason that high cone angle produces high buoyancy force, which leads to increased fluid movements and thus increased the average Nusselt number ($\bar{N}u$) with Rayleigh number (Ra) as expected. This increase is almost linear for Cone angles (C_A) 15 & 45 degrees.

© 2013 Global Journals Inc. (US)

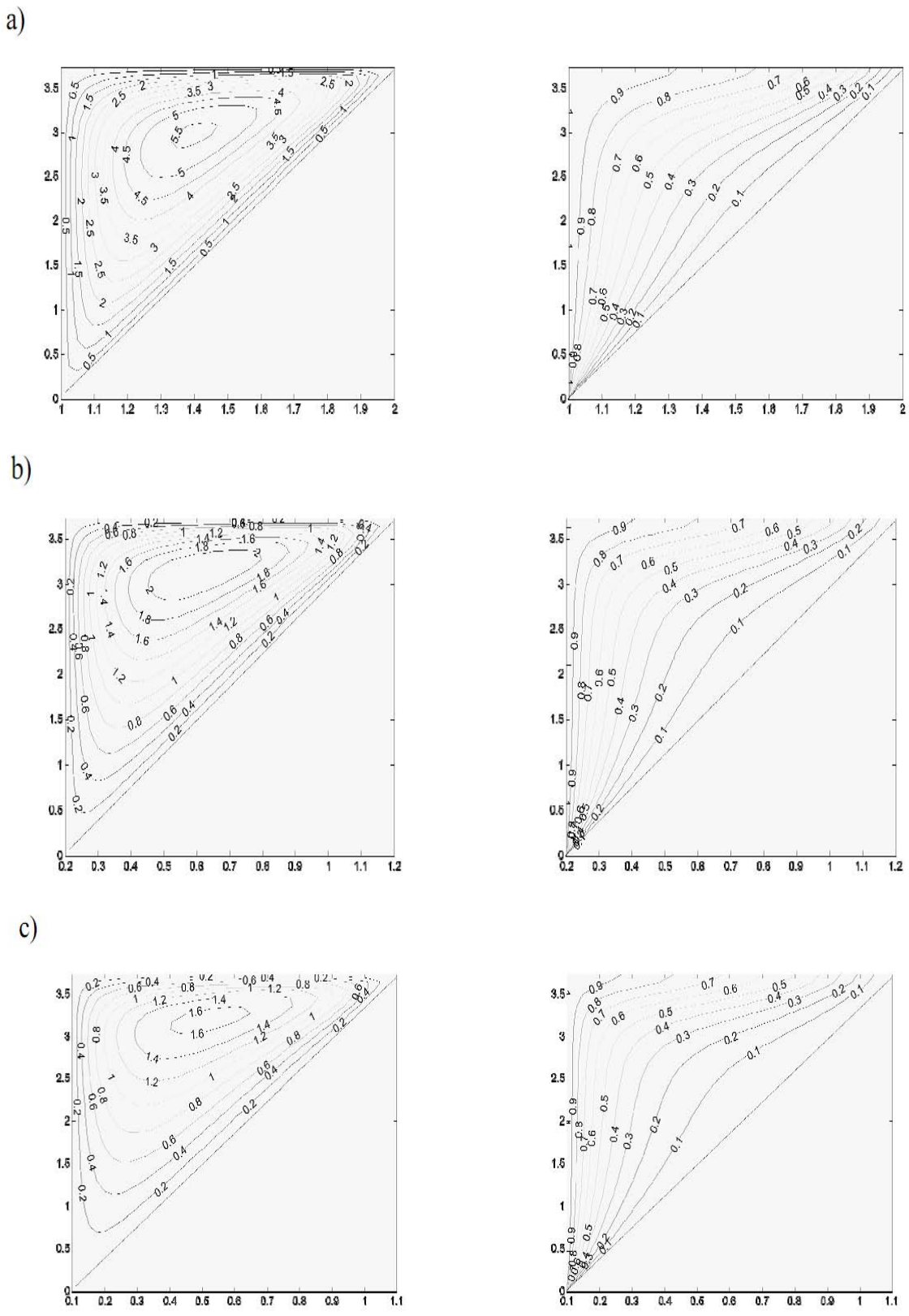

Figure 1.4.3 : Streamlines(left) and Isotherms(: Right) for Ra=50, C_A =15

a) R_r=1 b) R_r=5 c) R_r=10

© 2013 Global Journals Inc. (US)

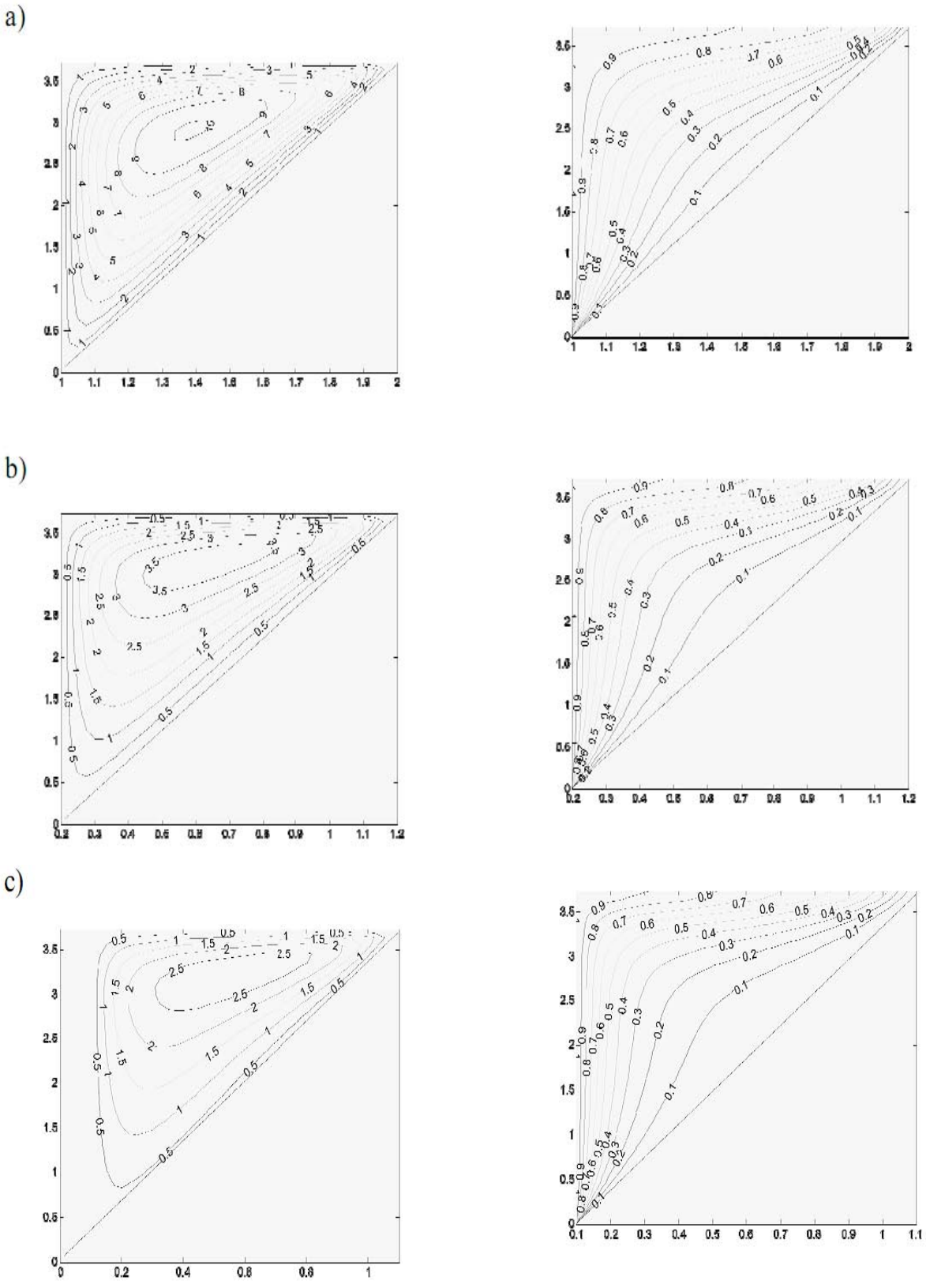

Figure 1.4.4 : Streamlines(left) and Isotherms(: Right) for Ra=100, C_A =15
a) R_r=1 b) R_r=5 c) R_r=10

© 2013 Global Journals Inc. (US)

Figure (1.4.4) shows the streamlines and isothermal lines inside the porous medium for various values of Radius ratio (R_r) at Ra = 50 and C_A = 15. It can be observed that be horizontal scale changes for various values of Radius Ratio (R_r). The magnitude of the streamlines decrease with the increase in Radius ratio (R_r). The thermal boundary layer thickness decreases with the increase in Radius ratio (R_r). It can be seen from the streamlines and isothermal lines that the fluid movement shifts from lower portion of the hot wall to the upper portion of the cold of the vertical annular cone with the increase in Radius ratio (R_r). The circulation of fluid covers almost whole domain at both lower and higher values of Radius ratio (R_r).

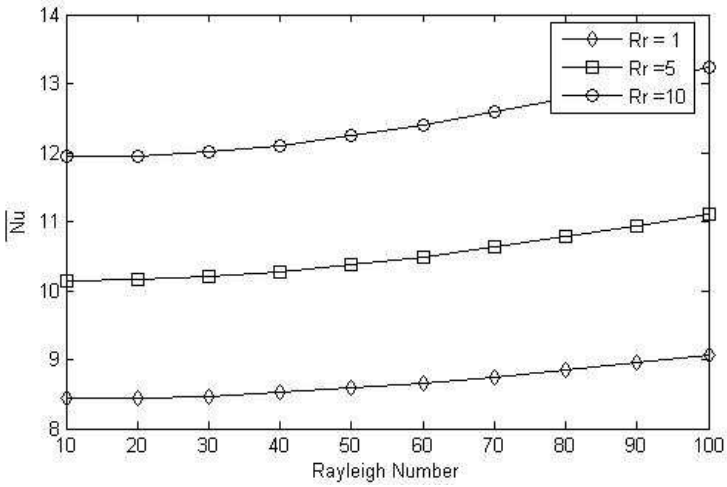

Figure 1.4.5 : $\bar{N}u$ variation with Ra at hot surface for different values of R_r at C_A = 75

Figure (1.4.5) shows the variation of average Nusselt number ($\bar{N}u$) at hot wall with respect to Rayleigh number (Ra). This Figure is obtained for the value of C_A = 75. When Radius ratio (R_r) is increased from 1 to 10 at the hot wall of the vertical annular cone, it is found that the average Nusselt number ($\bar{N}u$) at Ra = 10 is increased by 20%. The corresponding increases in average Nusselt number ($\bar{N}u$) at Ra = 100 is found to be 21%. The difference between the average Nusselt number ($\bar{N}u$) at two difference values of Radius ratio (R_r) increases with increase in Radius ratio (R_r). High Radius ratio (R_r) produces high buoyancy force, which leads to faster fluid movements and thus increased the average Nusselt number ($\bar{N}u$). i.e., for a given Rayleigh number (Ra) Nusselt number ($\bar{N}u$) increases with Radius ratio (R_r).

Figure (1.4.5) shows the streamlines and isothermal lines inside the porous medium for various values of Radius ratio (R_r) at Ra = 100 and C_A = 75. Though the value of Rayleigh number increases (Ra = 100), the streamlines and isothermal lines appears almost same as in Figure (1.4.7).

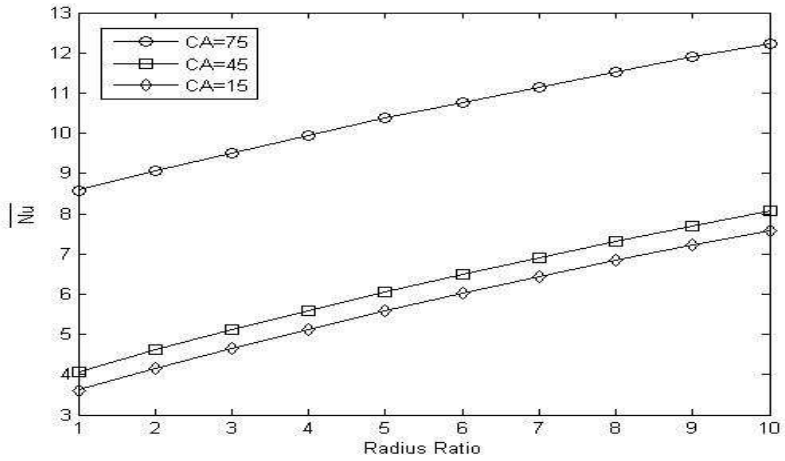

Figure 1.4.6 : $\bar{N}u$ variation with R_r at hot surface for different values of C_A at Ra = 50

© 2013 Global Journals Inc. (US)

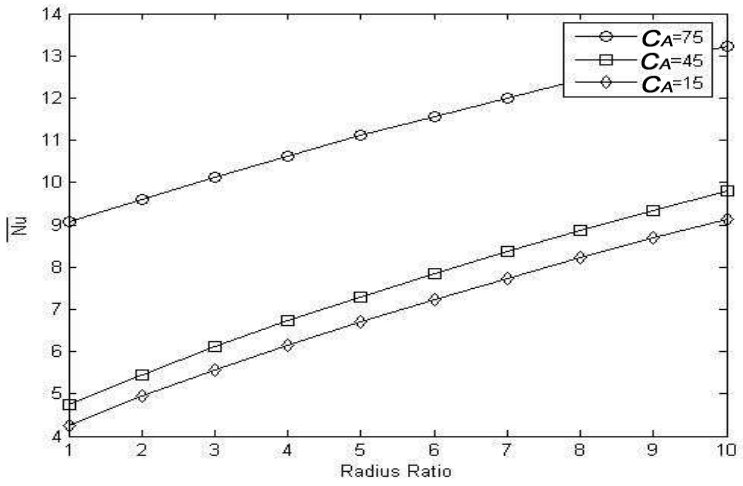

Figure 1.4.7 : $\bar{N}u$ variation with R_r at hot surface for different values of C_A at Ra = 100

Figure (1.4.7) illustrates the effect of Radius ratio (R_r) on average Nusselt number ($\bar{N}u$). This Figure corresponds to the value Ra = 50. It is seen that the average Nusselt number ($\bar{N}u$) at hot wall of the vertical annular cone increases with increase in Radius ratio (R_r). It is found that the average Nusselt number ($\bar{N}u$) at R_r = 1 increases by 9% when Cone angle (C_A) increased from 15 to 45. the corresponding increase in average Nusselt number ($\bar{N}u$) at R_r = 10 is found to be 9.4%. This difference becomes more prominent with the increase in Radius ratio (R_r) for higher values of cone angle. For a given Radius ratio (R_r) as the Cone angle (C_A) increases, the average Nusselt number ($\bar{N}u$) increases. The increase is marginal when the Cone angle (C_A) is increased from 15° to 45° when as we increases is substantial when we Cone angle (C_A) increases from 45° to 75°.

Figure (1.4.10) illustrates the effect of Radius ratio (R_r) on the average Nusselt number ($\bar{N}u$). This Figure corresponds to the value Ra = 100. It is seen that the average Nusselt number ($\bar{N}u$) at hot wall of the vertical annular cone increases with increase in Radius ratio (R_r). It is found that the average Nusselt number ($\bar{N}u$) at R_r = 1 increased by 9.2% when Cone angle (C_A) increased from 15 to 45. The corresponding increase in average Nusselt number ($\bar{N}u$) at R_r = 10 is found to be 9.8%. This difference between the average Nusselt number ($\bar{N}u$) at two different value of Cone angle (C_A) increases with increase Cone angle (C_A). This difference becomes more prominent with the increase in Radius ratio (R_r) for higher values of Cone angle (C_A).

a)

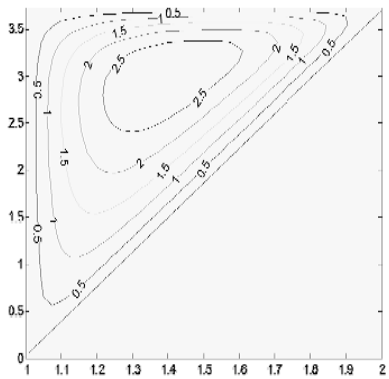

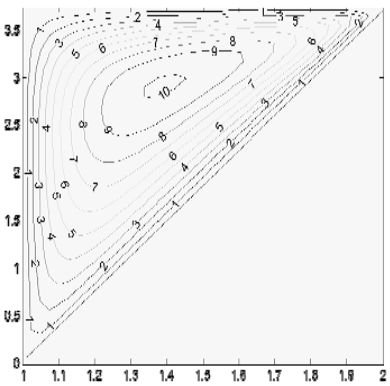

© 2013 Global Journals Inc. (US)

b)

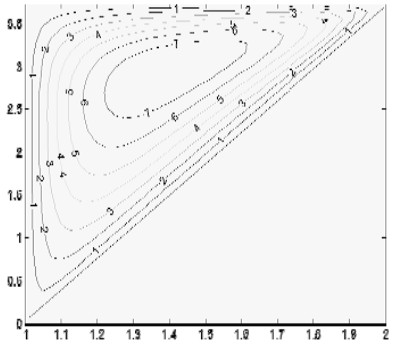

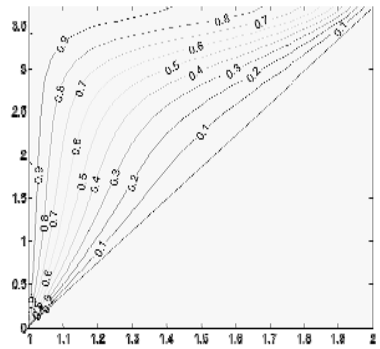

c)

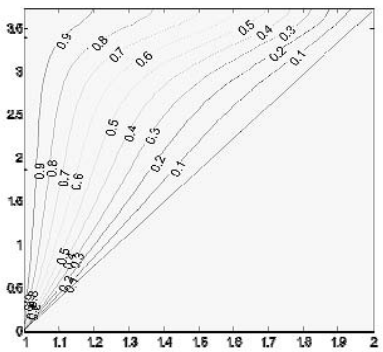

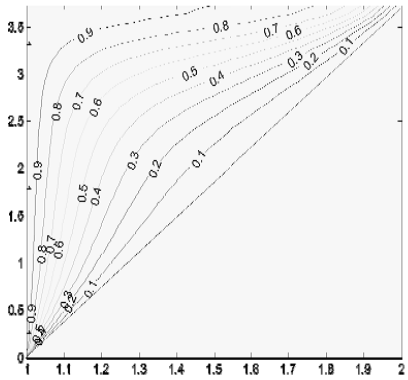

References Références Referencias

1. P. Cheng and W.J. Minkowycz, Journal of Geophysics. Res. 82 – 2040 (1977).
2. P. Cheng, Lett. Heat Mass Transfer 4, 119 (1977).
3. T.Y. Na and I. Pop, Int. J. Engng Sci. 21, 517 (1983).
4. R.S.R. Gorla A.H. Zinalabedini, ASME, J. Energy Resources Technology 109, 26(1987).
5. W.J. Minkowycz and P. Cheng, Int. J. Heat Mass Transfer-19, p. 805 (1976).
6. M.Kumari, I. Pop and G.Nath, Int. J. Heat mass Trasnfer-28, p–2171 (1985).
7. J.H. Merikin, Acta Mechanica 62, p-19, (1996).
8. A.P. Bassom and D.A.S. Ress, Acta Mechanica 116, 139 (1996).
9. P. Cheng, T.T. Le and I. Pop. Int. Comm. Heat Mass Transfer-12, p – 705 (1985).
10. P. Cheng, Into. J. Heat Mass Transfer-20, p – 201 (1977).
11. J.H. Merkin, Into. J. Heat Mass Transfer-21, p – 1499 (1978).
12. W.J. Minkowycz and P. Cheng. Lett Heat Mass Transfer-9, p–159 (1982).
13. A. Yücel, Num. Heat Transfer, 7, p – 483 (1984).
14. M.J. Hwang and C.K. Chen., ASME, J. Energy Resources Technology – 107, p –394 (1985).
15. A.A. Khan and A. Zebib, ASME J. Heat Trasnfer – 103 p – 179 (1981).
16. A. Raptis, G. Tzivanidis, and N. Kafoursias, Letter Heat Mass Transfer – 8, p – 417 (1981).
17. A. Bejan and K.R. Khair, Int, J. Heat Mass Transfer - 28, p – 909 (1985).
18. F.C. Lai and F.A. Kulacki, Int, J. Heat Mass Transfer - 34, p–1189 (1991).
19. A. Nakayama and M.A. Hossain, Int, J. Heat Mass Transfer - 38, p – 761 (1995).
20. P. Singh and Queeny, Acta Mechanica – 123, p – 69 (1997).
21. K.A. Yih, Acta Mechanica – 137, p – 83, (1999).
22. Trevisan O.V., Bejan A,: "Combined heat and mass Transfer by natural convection in a porous medium", Adv. Heat Transfer, Vol. 20 pp 315-352 (1990).
23. Bejan.A. Khair K.R,: "Heat and mass transfer by natural convection in a porous medium. Int, J. Heat Mass Transfer Vol - 28, pp 909 – 918 (1985).
24. Jang, J.Y., Chang W.J.: "Buoyancy – induced inclined boundary layer flow in a saturated porous medium resulting from combined heat and mass buoyancy effect". Int. comm. Heat Mass Transfer Vol - 15, pp 17 – 30 (1988).
25. Yücel., A., "Heat and mass transfer about vertical surfaces in saturated porous media". AICHE symposium series Vol - 85, pp 344 – 3349 (1989).
26. Yücel. A. "Natural convection heat and mass transfer along a vertical cylinder in porous medium."

© 2013 Global Journals Inc. (US)

Int, J. Heat Mass Transfer Vol - 33, pp 2265 – 2274 (1990).
27. Nakayama. A., Hossain, M.A., "An integral treatment for combined heat and mass transfer by natural convection in a porous medium. Int, J. Heat Mass Transfer Vol - 38, pp 761 – 765 (1995).
28. Singh. P., Queeny.O; "Free convection heat mass transfer along a vertical surface in a porous medium". Acta mech. Vol – 123, pp 69-73 (1997).
29. Lai. F.C; Choi, C.Y., Kulacki, F.A; "Coupled heat – and mass transfer by natural convection from slender bodies of revolution in porous media. Int. Comm. Heat Mass Transfer Vol - 17, pp 609–620 (1990).
30. Lai. F.C., Kulacki, F.A; "Coupled heat and mass transfer from a sphere buried in an infinite porous medium", Int, J. Heat Mass Transfer Vol - 33, pp 209 – 215 (1990).
31. Lai, F.C; "Coupled heat and mass transfer by natural convection from a horizontal line source in saturated porous medium". Int, comm. Heat Mass Transfer Vol - 17, pp 489 – 499 (1990).
32. Nakayama, A., Ashizawa. T., "A boundary layer analysis of combined heat and mass transfer by natural convection from a concentrated source in a saturated porous medium". Appl. Sci. Res – 56, pp – 1-11, (1996).
33. A. Bejan, "Convective Heat Transfer", 2nd Edition, New York, John Wiley & Sons (1995).
34. R.W. Lewis, P. Nithiarasu and K.N. Seetharamu "Fundamentals of the finite element method for heat and fluid flow. John Wiley and Sons, Chichester (2004).
35. L.J. Seger land, "Applied Finite Element Analysis" John Wiley & Sons, New York (1982).
36. R.W. Clugh, "The Finite Element Analysis in plane stress Analysis" Proc. 2nd ASCE conf. on Electronic computation, Pittsburg, PA.
37. O.C. Zinkiewicz and K. Cheng, "Finite Element in the solution of field problems" Engineer, Vol 200, pp, 507-510 (1965).

© 2013 Global Journals Inc. (US)